NASA TECHNICAL NOTE

NASA TN D-2121

NASA TN D-2121

CORRELATION OF A TURBULENT AIR-BROMINE COAXIAL-FLOW EXPERIMENT

by Robert G. Ragsdale, Herbert Weinstein, and Chester D. Lanzo

Lewis Research Center
Cleveland, Ohio

NATIONAL AERONAUTICS AND SPACE ADMINISTRATION • WASHINGTON, D. C. • FEBRUARY 1964

CORRELATION OF A TURBULENT AIR-BROMINE COAXIAL-FLOW EXPERIMENT

By Robert G. Ragsdale, Herbert Weinstein,
and Chester D. Lanzo

Lewis Research Center
Cleveland, Ohio

NATIONAL AERONAUTICS AND SPACE ADMINISTRATION

For sale by the Office of Technical Services, Department of Commerce,
Washington, D.C. 20230 -- Price $1.00

CORRELATION OF A TURBULENT AIR-BROMINE COAXIAL-FLOW EXPERIMENT

SUMMARY

A previously published laminar analysis of an isothermal coaxial-flow system is extended to turbulent flow. Mixing-length theory is used to develop a general expression for a dimensionless eddy viscosity. Experimental data were obtained for a slow-moving bromine stream injected into a fast-moving air stream. Axial variations of average bromine concentration were measured optically for air Reynolds numbers from 1330 to 49,300, bromine Reynolds numbers from 255 to 3850, and air-to-bromine initial-velocity ratios from 0.83 to 0.97 and 1.25 to 49.

For the lowest bromine Reynolds number of 255, an air Reynolds number of 1730, and an initial-velocity ratio of 4.3, the data were in agreement with the laminar analysis. For all other runs, the data were well represented by introducing a value of the dimensionless eddy viscosity ϵ^+ into the analysis to account for turbulence. The turbulence factors obtained by curve fitting the data were correlated within ±25 percent as the following function of the initial outer- to inner-stream velocity ratio $\bar{u}_2$ and the initial inner-stream Reynolds number,

$$\epsilon^+ = 0.0172\left|\bar{u}_2 - 1\right|^{1/2}(Re_{1,0} - 250)$$

where $0.83 \leq \bar{u}_2 \leq 0.97$, $1.25 \leq \bar{u}_2 \leq 49$, and $255 \leq Re_{1,0} \leq 3850$.

INTRODUCTION

An interesting and complex fluid mechanics problem arises when one gas is injected into a different surrounding gas that is flowing in the same direction. Subsonic coaxial-jet mixing occurs in such practical instances as ejectors, afterburners, and combustion chambers, as well as in more advanced situations found in plasma injection systems (ref. 1) and gaseous nuclear rocket concepts (ref. 2).

What is desired in each case is an understanding of the basic mass, the momentum, and the energy interchanges that occur between the two coaxially flowing streams. The general flow pattern of interest is illustrated in figure 1. The number and the complexity of the exchange mechanisms that transpire in the region of fluid interaction depend on the initial conditions of the two fluids.

For a one-component isothermal system, momentum transfer will be present if the two streams move at different initial velocities. This is the simplest case,

and it has been treated both analytically and experimentally in a relatively straightforward manner as reported in reference 3. If the two streams are not of the same fluid, mass transfer will take place by molecular and/or turbulent diffusion. If the two fluids are of substantially different molecular weights, the analytical method of reference 3 is not applicable; an analytical treatment of the two-fluid problem is presented in reference 4 for laminar flow. Finally, thermal-energy transport will occur if the two streams are at initially different temperatures, or if there is internal heat generation in one or both of the fluids. Some velocity and temperature profile data are presented in reference 5 for hot air injected coaxially into cold air.

Though the analysis of reference 4 can be applied to the laminar, isothermal coaxial flow of any two fluids, for the more frequently encountered regime of turbulent flow, additional information is required about the local variation of turbulence. Certain simplified flow models such as mixing-length theory can be used to formulate turbulent flow forms of the laminar relations, but this gives rise to unknown correlation coefficients, exponents, proportionality constants, and the like. In short, additional experimental information is needed for two-component coaxial-flow systems.

Most of the jet mixing work reported previously is concerned with a "free jet" of fluid issuing into a stagnant environment of the same fluid. Reference 6 gives a partial bibliography of such studies and presents experimental data for the mixing of an air-air system. Different stream densities were obtained by preheating one air stream, and, therefore, the data are not for a two-fluid system. The data obtained were for outer- to inner-stream initial-velocity ratios from 0.25 to 0.75 and density ratios from 0.62 to 1.16.

Reference 7 reports an analysis of one stream issuing into another surrounding stream of different velocity. Turbulence is accounted for by assuming a mixing length proportional to the width of the mixing region. The integrated momentum analysis of reference 7 utilizes velocity profiles that are assumed similar (cosine shaped) at all axial positions. Comparing the analysis of reference 7 with the experimental data of reference 6, the authors of reference 6 concluded that the analysis is only valid for small density differences.

Experimental data for turbulent mass transfer in a coaxial-flow system are presented in reference 8. Radial concentrations were measured at various axial positions by a probe technique. The study was restricted to a molecular-weight ratio near unity (air and natural gas were used), and data were obtained only for an average outer- to inner-stream velocity ratio of unity. The data are used to compute an eddy diffusivity, which the authors concluded decreases with increasing distance from the injection point and reaches a minimum value at a section 10 to 25 injection diameters downstream from the point of initial mixing. In addition, the magnitude of eddy diffusivity at a particular point in the turbulent stream is roughly proportional to the Reynolds number.

Reference 9 summarizes some coaxial-flow studies conducted on the turbulent transfer of momentum, mass, and temperature. The onset of turbulence is graphically illustrated by pictures obtained with a high-speed spark shadowgraph. The results of various mixtures of helium and carbon dioxide injected into air indicate that the mixing rate of the two streams is dependent primarily on the

initial-velocity ratio rather than on the velocity difference. Probe measurements indicate that mass and temperature diffuse at the same rate, which is greater than the rate of turbulent momentum diffusion. Some analytical results of the analysis of reference 7 are also shown in reference 9.

The laminar analysis of reference 4 is most applicable to a two-fluid coaxial-jet system and was extended to include turbulence effects by introducing a dimensionless eddy viscosity. An air-bromine test setup was constructed at the Lewis Research Center to obtain experimental data on the mixing of a two-fluid coaxial-flow system. The turbulent modification of the analysis and a limited amount of concentration data are reported in reference 10.

This report is an extension of the work reported in reference 10. The goal of this study is twofold. The first objective is to determine whether the modified laminar analysis can be made to describe the turbulent mixing process in a two-fluid coaxial-flow system by selecting a dimensionless eddy viscosity, over a wide range of initial-velocity ratios and Reynolds numbers. The second purpose is to correlate the dimensionless eddy viscosities thus obtained in terms of physical parameters such as initial-velocity ratio and Reynolds numbers.

Experimental measurements of concentration were obtained for the isothermal, coaxial flow of a heavy, slow-moving inner stream of bromine injected into a light, fast-moving outer stream of air. By a systematic variation of air and bromine flow rates, the data of reference 8 are herein extended to cover a range of air-to-bromine initial-velocity ratios from 0.83 to 49. For each run, radial average bromine concentrations were optically measured at various axial distances downstream from the injection point. A mixing-length model of turbulent coaxial flow is used to obtain an expression relating a dimensionless eddy viscosity to initial conditions. The form of this expression is then used to obtain a correlation of the indicated dimensionless eddy viscosities.

SYMBOLS

a	acceleration
b	width of mixing region
C	mole fraction of inner-stream component
C^*	normalized bromine concentration, eq. (18)
D	molecular diffusion coefficient
$D_{1,1}$	self-diffusion coefficient of inner stream
$D_{1,2}$	binary diffusion coefficient
E	extension coefficient
F	initial inner-stream Froude number, u^2/ar
f	general function

h/h_o	deflection ratio
K	proportionality constant
M	molecular weight
P	general transport property, eq. (4)
Re	Reynolds number, $2ru\rho/\mu$
r	radial coordinate
r_o	inner-stream radius at z = 0
r_w	dimensionless distance to outer wall
Sc	Schmidt number, $\mu/\rho D$
T	temperature
u	axial velocity component
V	molecular volume
v	radial velocity component
z	axial coordinate
$\bar{z}$	dimensionless axial distance, z/r_o
β	molecular weight parameter, $(M_1/M_2) - 1$
ϵ	eddy diffusivity
ϵ^+	dimensionless eddy viscosity, $\rho\epsilon/\mu$
μ	viscosity
$\bar{\mu}_2$	ratio of outer- to inner-stream viscosities
ρ	density
ψ	stream function

Subscripts:

max	maximum
min	minimum
mix	mixture
ref	reference

t turbulent

0 initial face, z = 0

1 inner stream

2 outer stream

Superscripts:

' dummy integration variable

$\bar{}$ normalized to inner-stream value at z = 0

* normalized to inner-stream value at $z = z_{ref}$

ANALYSIS

The laminar analysis presented in reference 4, which is the basis of the present work, is summarized here. The extension of the basic analysis to include turbulence effects, presented in reference 10, is also included along with some enlargement and modifications. A mixing-length model of a coaxial-flow system is used to develop an expression for a dimensionless eddy viscosity in terms of pertinent physical parameters.

Laminar Flow

The analysis is based on the model shown in figure 2 and yields radial concentration and velocity profiles at various axial distances downstream from the injection point. Solutions are obtainable for any initial concentration and velocity profiles - step, ramp, or continuous.

The assumptions and restrictions inherent in the analysis are:

(1) The entire flow field is steady state and at constant temperature and pressure.

(2) Axial symmetry exists.

(3) The fluids mix ideally; there is no volume or temperature change due to mixing.

(4) The usual boundary-layer assumptions apply: $\frac{\partial u}{\partial r} \gg \frac{\partial u}{\partial z}$; $u \gg v$; $\frac{\partial \psi}{\partial r} \gg \frac{\partial \psi}{\partial z}$.

(5) The flow is incompressible.

(6) The dimensionless eddy viscosity ϵ^+ is constant throughout the flow field (used in turbulent extension of analysis).

The method of reference 4 is numerical in nature. An equation set is derived and is integrated from the initial face at the fluid entrance in the downstream direction through the region of interest to an arbitrary end point. To

make the problem an initial-value one, the walls are not included in the problem, and the outer, or air, stream is considered infinite in radial extent. This introduces little error in this case since, for the region of interest, the mixing process does not approach the wall.

The equation set consists of the continuity equation with the steady-state and axial-symmetry assumptions; the momentum equation, which is the axial-component Navier-Stokes equation including the body force term, with boundary-layer, steady-state, axial-symmetry, constant-pressure, and constant-temperature assumptions; and the diffusion equation, with axial-symmetry and steady-state assumptions. These three equations are taken through a transformation to an axial-length stream-function coordinate set.

The dimensional equation set is:

Continuity:

$$\frac{\partial}{\partial r}(\rho v r) + \frac{\partial}{\partial z}(\rho u r) = 0$$

Momentum:

$$v\frac{\partial u}{\partial r} + u\frac{\partial u}{\partial z} = \frac{1}{\rho r}\frac{\partial}{\partial r}\left(r\mu\frac{\partial u}{\partial r}\right) + \frac{a(\rho - \rho_2)}{\rho}$$

Diffusion:

$$v\frac{\partial C}{\partial r} + u\frac{\partial C}{\partial z} = \frac{\rho}{r}\frac{\partial}{\partial r}\left(\frac{rD_{1,2}}{\rho}\frac{\partial C}{\partial r}\right)$$

These are made dimensionless by the introduction of the following terms:

$$\beta = \frac{M_1}{M_2} - 1, \quad \rho = \rho_2(\beta C + 1)$$

$$\bar{D} = \frac{D_{1,2}}{D_{1,1}} \qquad \bar{r} = \frac{r}{r_0} \qquad \bar{u} = \frac{u}{u_{1,0}}$$

$$\bar{z} = \frac{z}{r_0} \qquad F = \frac{u_{1,0}^2}{r_0 a} \qquad \bar{v} = \frac{v}{u_{1,0}}$$

$$\bar{\mu} = \frac{\mu}{\mu_1} \qquad \frac{Re_{1,0}}{2} = \frac{r_0 u_{1,0}\rho_{1,0}}{\mu_{1,0}} \qquad Sc_{1,0} = \frac{\mu_{1,0}}{\rho_{1,0}D_{1,1}}$$

The dimensionless equations are:

Continuity:

$$\frac{\partial}{\partial \bar{r}}\left[\overline{rv}(\beta C + 1)\right] + \frac{\partial}{\partial \bar{z}}\left[\overline{ru}(\beta C + 1)\right] = 0$$

Momentum:

$$\bar{v}\frac{\partial \bar{u}}{\partial \bar{r}} + \bar{u}\frac{\partial \bar{u}}{\partial \bar{z}} = \frac{2}{Re_{1,0}}\frac{\beta + 1}{\beta C + 1}\frac{1}{\bar{r}}\frac{\partial}{\partial \bar{r}}\left(\overline{\mu r}\frac{\partial \bar{u}}{\partial \bar{r}}\right) + \frac{\beta C}{F(\beta C + 1)}$$

Diffusion:

$$\bar{v}\frac{\partial C}{\partial \bar{r}} + \bar{u}\frac{\partial C}{\partial \bar{z}} = \frac{2}{Re_{1,0}Sc_{1,0}}\frac{\beta C + 1}{\bar{r}}\frac{\partial}{\partial \bar{r}}\left(\frac{\overline{Dr}}{\beta C + 1}\frac{\partial C}{\partial \bar{r}}\right)$$

The stream function ψ is defined by the following relations:

$$\frac{\partial \psi}{\partial \bar{z}} = -(\overline{rv})(\beta C + 1)$$

$$\frac{\partial \psi}{\partial \bar{r}} = (\overline{ru})(\beta C + 1)$$

This satisfies the dimensionless continuity equation.

The dimensionless equation set is transformed to the $z - \psi$ coordinate space, and the following relations result:

Momentum:

$$\frac{\partial \bar{u}}{\partial \bar{z}} = 2\frac{\beta + 1}{Re_{1,0}}\frac{\partial}{\partial \psi}\left[\overline{\mu r^2}\bar{u}(\beta C + 1)\frac{\partial \bar{u}}{\partial \psi}\right] + \frac{\beta C}{F_{1,0}\bar{u}(\beta C + 1)} \tag{1}$$

Diffusion:

$$\frac{\partial C}{\partial \bar{z}} = \frac{2(\beta C + 1)^2}{Re_{1,0}Sc_{1,0}}\frac{\partial}{\partial \psi}\left[\overline{Dr^2}\bar{u}\frac{\partial C}{\partial \psi}\right] \tag{2}$$

Continuity:

$$\int_0^{\bar{r}} \bar{r}'\,\overline{dr}' = \int_0^{\psi} \frac{1}{\bar{u}(\beta C + 1)}\,d\psi' \tag{3}$$

This is the form in which the equations are integrated.

The transport properties of the fluid mixtures are evaluated from the pure-component fluid properties with an elementary mixing law (ref. 11):

$$P_{mix} = \frac{CM_1 + (1 - C)M_2}{\frac{CM_1}{P_1} + \frac{(1 - C)M_2}{P_2}} \tag{4}$$

Application of this law to the viscosity yields:

$$\bar{\mu} = \frac{\beta C + 1}{(\beta + 1)C + \frac{1 - C}{\bar{\mu}_2}} \tag{5}$$

where $\bar{\mu}_2$ is the ratio of the outer- to inner-stream viscosities.

The dimensionless binary diffusion coefficient, because it is assumed invariant with concentration, is evaluated from manipulation of the Gilliland equation (ref. 12):

$$\bar{D} \equiv \frac{D_{1,2}}{D_{1,1}} = \frac{2\sqrt{2(\beta + 2)}}{\left(1 + \bar{V}_2^{1/3}\right)^2} \tag{6}$$

where $D_{1,1}$ is the self-diffusion coefficient of the inner stream and $D_{1,2}$ is the binary diffusion coefficient. The molecular-volume ratio, air to bromine, is obtained from values given in reference 12:

$$\bar{V}_2 = \frac{29.9}{2(27.0)} = 0.554$$

The viscosity ratio, air to bromine, is taken from reference 13 for 70° F:

$$\bar{\mu}_2 = \frac{1.2 \times 10^{-5}}{0.988 \times 10^{-5}} = 1.22$$

The bromine Schmidt number is calculated from these properties:

$$Sc = \frac{\mu_1}{\rho_1 D_{1,1}}$$

The self-diffusion coefficient is given by the Gilliland equation as

$$D_{1,1} = \frac{2.62 \times 10^{-6} \sqrt{2TM_1}}{\left(2V_1^{1/3}\right)^2 \rho_1}$$

This gives the Schmidt number as

$$Sc_{1,0} = \frac{0.988 \times 10^{-5}}{1.885 \times 10^{-5}} = 0.526$$

Equations (1), (2), (3), (5), and (6) comprise the set that is integrated numerically from initial slug-velocity and concentration profiles to a specified end point in the axial direction corresponding to the length of the experimental

test section, about $\bar{z} = 30$. A detailed description of the numerical technique and the computer program is given in reference 4.

As described in the following section, the data obtained from the experiment are a measure of the number of bromine molecules along a diameter of the test section at a given axial position. This pseudo-concentration is normalized to a reference axial station at the first data-point location. A corresponding value of this relative bromine concentration is computed in the program by

$$C^* = \frac{\int_0^{\bar{r}_w} C \, d\bar{r}}{\int_0^{\bar{r}_w} C \, d\bar{r}\Big|_{\bar{z}=\bar{z}_{ref}}} \tag{7}$$

Turbulent Flow

The laminar analysis is extended to include turbulent flow by substituting the turbulent transport properties for the laminar ones. This is done in the usual manner:

$$\begin{aligned} \mu_t &= \mu(1 + \epsilon^+) \\ D_t &= D\left(1 + \frac{\epsilon}{D}\right) \end{aligned} \tag{8}$$

where ϵ^+ is the ratio of turbulent to laminar viscosity, $\rho\epsilon/\mu$. This ratio is assumed to be constant with both radius and axial location as in Schlicting (ref. 14).

With the assumption that the mixing law given by equation (4) applies to turbulent properties, equations (4) and (8) give the turbulent transport properties as

$$\bar{\mu}_t = \frac{\beta C + 1}{\frac{(\beta + 1)C}{1 + \epsilon^+} + \frac{(1 - C)}{(1 + \epsilon^+)\bar{\mu}_2}} \tag{9}$$

and

$$\bar{D}_t = \frac{\beta C + 1}{\frac{(\beta + 1)C}{\bar{D} + \epsilon^+ Sc} + \frac{(1 - C)}{\bar{D} + \epsilon^+ \bar{\mu}_2 Sc_{1,0}(\beta + 1)}} \tag{10}$$

It can be seen that a constant ϵ^+ does not imply constant transport properties in the mixing region; $\bar{\mu}_t$ and $\bar{D}_t$ will vary with concentration in both the radial and the axial directions. The turbulent flow calculations are made with equations (1), (2), (3), (9), and (10), and the integration is done in the same manner as for laminar flow.

Coaxial Mixing-Length Model

The extension of the laminar analysis to turbulent flow introduces a required but unknown quantity ϵ^+. A mixing-length model for a coaxial-flow system was used to develop an expression for this quantity in terms of physically known or measurable parameters. The argument is as follows.

For the case of free turbulent flow (no wall effects present), Prandtl postulated that the turbulent eddy size is the same order of magnitude as the width of the mixing region (ref. 14, p. 481). For an eddy diffusivity that is proportional to the maximum velocity difference across the mixing region, this postulate leads to

$$\epsilon = Kb(u_{max} - u_{min}) \tag{11}$$

where b is the width of the mixing zone, and K is a proportionality constant to be determined from experimental information. For a single-fluid system, ϵ can be assumed constant over the entire flow field (ref. 14, p. 592).

It is herein assumed that the width of the mixing region is proportional to the initial inner-stream radius and that the velocity difference in equation (11) can be represented by its value at the injection point. With these assumptions equation (11) can be written in terms of a dimensionless eddy viscosity ($\rho\epsilon/\mu$):

$$\epsilon^+ \equiv \left(\frac{\rho\epsilon}{\mu}\right) = K\left(\frac{\rho r_0}{\mu}\right)|u_{2,0} - u_{1,0}| \tag{12}$$

The absolute value of the velocity difference is used to include the case where the inner stream initially moves faster than the outer one. This expression can also be written in terms of the initial inner-stream Reynolds number and the velocity ratio at the injection point:

$$\epsilon^+ = \frac{\left(\frac{K}{2}\right)|\bar{u}_2 - 1|Re_{1,0}}{\left(\frac{\mu}{\mu_1}\right)\left(\frac{\rho_1}{\rho}\right)} \tag{13}$$

For incompressible flow of an isothermal single-fluid system, the viscosity and density ratios in equation (13) drop out. For a two-component system, however, this is not the case. The entire flow field can be characterized by a single constant value of ϵ^+, but the point of evaluation must first be chosen.

It can be postulated that the turbulence is initiated in the outer stream and then propagated throughout the inner stream. This assumption yields equation (13) as

$$\epsilon^+ = \frac{\left(\frac{K}{2}\right)|\bar{u}_2 - 1|Re_{1,0}}{\bar{\mu}_2(1 + \beta)} \tag{14}$$

If ϵ^+ is evaluated in the inner stream, the property ratios drop out and equation (13) becomes

$$\epsilon^+ = \left(\frac{K}{2}\right)|\bar{u}_2 - 1|Re_{1,0} \tag{15}$$

For the purpose of correlating the data of this report, either equation (14) or (15) will suffice with equal facility; since only one isothermal system, air-bromine, was used, the property ratios $\bar{\mu}_2$ and $(1 + \beta)$ are constant while $Re_{1,0}$ and $\bar{u}_2$ are the only variables. The form of equation (15) was used to correlate the air-bromine data. Additional data for the coaxial mixing of other two-component systems (different fluids) will be necessary to disclose the effect of properties on dimensionless eddy viscosity.

The main value of equation (15) is to guide data correlation; that is, to suggest the functional dependence of the dimensionless eddy viscosity on pertinent parameters. To this end, equation (15) simply indicates that the dimensionless eddy viscosity is a function of the inner-stream initial Reynolds number and the initial-velocity ratio:

$$\epsilon^+ = f_1|\bar{u}_2 - 1|f_2(Re_{1,0}) \tag{16}$$

APPARATUS AND PROCEDURE

Experimental Apparatus

The air-bromine coaxial-flow test apparatus is shown schematically in figure 3. Dry air is metered by a parallel orifice and rotameter system, is introduced through a tube bundle to remove large-scale turbulence, and then flows downward through a 5- by 5-inch Lucite channel. Bromine vapor is generated in a boiler, is passed through a rotameter, and is then injected into the airstream 2 feet downstream from the tube bundle through a 0.43-inch inside diameter Monel tube. The test section was operated at the vapor pressure of room temperature bromine (approx. 4 lb/sq in. abs). A photograph of the test section is shown in figure 4. Bromine flow rate was changed by varying electrical power to the boiler. Runs were made by setting the air flow rate and then by varying the bromine flow rate over the possible range. This process was repeated for several air flow rates.

Instrumentation

Average bromine concentrations were measured by an optical light absorption method. By means of a mirror arrangement, a single light source was used to produce eight collimated light beams that were 1/8 inch in diameter and 1 inch apart. These light beams were passed through the bromine stream along a diameter, where the first station is at the injection point. The light beams were passed through a 50-angstrom band-pass interference filter with peak transmission at 4150 angstroms, a wavelength at which bromine is highly absorptive. The intensity of the transmitted light was then measured by eight photomultiplier

detectors, and the outputs were recorded on a multichannel light-beam oscillograph.

Each channel was adjusted by resistance damping to have approximately the same full-scale (unattenuated light-beam) deflection. For each run, oscillograph readings were taken before, during, and after bromine flow. Typical output is shown in figure 5; axial station A is at the injection point and H is the farthest downstream. A photomultiplier located in the light box was used periodically to monitor the intensity of the source.

Data Reduction

With the assumption of linearity of the oscillograph, the ratio of attenuated to full-scale deflection is also the intensity ratio of the light beam. The deflection ratio h/h_o is related to the concentration of attenuating material by Beer's law:

$$\frac{h}{h_o} = e^{-EC} \tag{17}$$

The extinction coefficient E is eliminated by normalizing each measured deflection ratio to that of the first station to obtain a relative bromine concentration:

$$C^* = \frac{\ln\left(\frac{h}{h_o}\right)}{\ln\left(\frac{h}{h_o}\right)_{ref}} \tag{18}$$

The measurements thus obtained represent the number of bromine molecules in the light path (which would be proportional to the integral of $C\,dr$) and do not represent a true radial average (which would be proportional to the integral of $Cr\,dr$). The same pseudo-average concentration was calculated numerically with equation (7). The experimental data are given in tables I and II.

RESULTS AND DISCUSSION

Accuracy and Limitations

Experimentally determined values of normalized bromine concentration at various axial stations were obtained over a range of air and bromine flow rates. The experimentally obtainable flow rates resulted in the following ranges: air Reynolds number, 1330 to 49,300; bromine Reynolds number, 255 to 3,850; and air-to-bromine velocity ratio, 0.83 to 49.

For each run, initial experimental conditions were used as input to the analytical computer program. Values of the dimensionless eddy viscosity ϵ^+ were chosen arbitrarily to generate a family of curves to bracket the data. The value of ϵ^+ was taken as the one that best fitted the data. Figure 6 illustrates the sensitivity of the analytical solution to the dimensionless eddy

viscosity for run 10 ($\epsilon^+ = 30$).

Laminar Flow

Since there is no established critical Reynolds number for coaxially flowing fluids, the term "laminar" flow of a coaxial system must be used with care. It is used herein to mean that the data agreed with the laminar analysis ($\epsilon^+ = 0$). In that sense, one laminar run was obtained, and the data are shown in figure 7. The analytical solutions for laminar flow ($\epsilon^+ = 0$) and for $\epsilon^+ = 1$ are shown as solid lines.

This run, run 5, was for the lowest bromine flow that was experimentally possible. The bromine Reynolds number was 255, the air Reynolds number was 1730, and the air-to-bromine initial-velocity ratio was 4.3. Since only one set of data was obtained that agreed with the laminar analysis, no general conclusions can be drawn about laminar flow criteria. The agreement shown in figure 7 does indicate, however, that the basic laminar analysis properly describes the flow pattern that exists at relatively low Reynolds numbers. This gives no indication of what conditions are necessary to achieve this "laminar" mixing of coaxial streams. The low data point at the second station ($\bar{z} = 4.65$) is attributed to a photomultiplier misalignment and not to an actual flow characteristic.

Turbulent Flow

With the exception of the run just discussed, a value of ϵ^+ greater than zero was required to get analytical agreement with the data. As seen in figure 6, the data fall considerably below the laminar prediction.

Figure 8 shows some typical runs to illustrate the agreement between the data and the turbulent analysis for a number of conditions. The analytical results shown as solid lines are for the ϵ^+ that best fitted the data.

The significant conclusion indicated by figure 8 is that the effect of turbulence appears to be properly included in the analysis. Although the analytical curves can be adjusted by selecting various values of ϵ^+, the general shape of the curves remains the same and agrees well with the experimental results. As the initial-velocity ratio increases, the trend of the data depart somewhat from the analysis, as is shown in figures 8(f) and (g). The data fall below the calculated line at a $\bar{z}$ of about 5 and above it for $\bar{z}$'s of 20 to 30. The data in figure 8(h) have the same trend although it is not readily discernable because of the scale used. Such a trend may be due to an axial variation of ϵ^+, a condition not included in the analytical curves. The agreement of the analysis and experiment is quite satisfactory, a fact that lends credence to the assumed constancy of ϵ^+.

A series of runs was made for a constant air Reynolds number and a varying bromine flow rate to investigate the effect of initial-velocity ratio. Four such runs are shown in figure 9(a) for a constant air Reynolds number of 16,600. The solid lines again represent the best fit and are for the ϵ^+ values shown.

It is important to note that decreasing the bromine flow rate at constant air flow rate not only increased the air-to-bromine initial-velocity ratio, but also decreased the initial bromine Reynolds number. The form of equation (16) indicates that an increase of initial-velocity ratio should increase the dimensionless eddy viscosity, but that a decrease of the initial bromine Reynolds number should decrease it. The data shown in figure 9(a) indicate that the result of these opposing influences is to decrease the dimensionless eddy viscosity as the bromine flow rate is reduced. This suggests that the dimensionless eddy viscosity is a stronger function of inner-stream Reynolds number than of initial-velocity ratio.

Figure 9(b) shows the effect of varying the initial-velocity ratio at a nearly constant bromine Reynolds number. This variation of initial-velocity ratio is therefore accompanied by a changing air stream flow rate or Reynolds number. As the velocity ratio increases from 1.7 to 9 and the corresponding air Reynolds numbers vary from 8680 to 45,100, the dimensionless eddy viscosity varies from 43 to 140. Thus two conclusions are indicated by figures 9(a) and (b). First, for constant air stream conditions, a decrease of bromine flow rate, which has the dual effect of increasing the air-to-bromine initial-velocity ratio and decreasing the bromine initial Reynolds number, results in a decrease of turbulence as measured by the dimensionless eddy viscosity. Second, for constant bromine stream conditions, an increase of air flow rate, which increases both the initial-velocity ratio and the air Reynolds number, increases the turbulence.

Correlation of Data

The expression for dimensionless eddy viscosity derived from a mixing-length model was used as a guide to obtain a correlation of ϵ^+ in terms of pertinent physical parameters. The relation obtained was

$$\epsilon^+ = f_1|\bar{u}_2 - 1|f_2(\mathrm{Re}_{1,0}) \tag{16}$$

It was first assumed that $f_2(\mathrm{Re}_{1,0})$ was simply $\mathrm{Re}_{1,0}$, and therefore the velocity ratio function $|\bar{u}_2 - 1|$ was plotted against the ratio $\epsilon^+/\mathrm{Re}_{1,0}$ in figure 10. The data points are represented by the solid line that has a slope of 1/2. Thus, in the first approximation, equation (16) has the form

$$\epsilon^+ = |\bar{u}_2 - 1|^{1/2} f_2(\mathrm{Re}_{1,0})$$

Based on this indication, the data were next plotted as $\epsilon^+/|\bar{u}_2 - 1|^{1/2}$ against $\mathrm{Re}_{1,0}$ to determine the form of $f_2(\mathrm{Re}_{1,0})$ (fig. 11). The data are well represented by a straight line on this rectilinear plot. The line that appears to best fit the data does not go through the origin, however, but instead intersects the abcissa at about $\mathrm{Re}_{1,0} = 250$. This does not imply any particular significance as to a transition Reynolds number, but is just the numerical result of

an empirical correlation of the data. When this information from figure 11 is used the form of equation (16) is

$$\epsilon^+ = |\bar{u}_2 - 1|^{1/2}(Re_{1,0} - 250)$$

Since this is not consistent with the assumed Reynolds number dependency that led to the exponent of 1/2 on the velocity-ratio function, the data were replotted as $\epsilon^+/(Re_{1,0} - 250)$ against $|\bar{u}_2 - 1|$. Figure 12 shows that the same exponential dependency on initial-velocity ratio exists. The solid line drawn through the data still has a slope of 1/2.

The final correlation of the data is shown in figure 13, represented within about ±25 percent by

$$\epsilon^+ = 0.0172|u_2 - 1|^{1/2}(Re_{1,0} - 250)$$

Though it becomes a little tedious, it is necessary to restrict this correlation to the ranges established by the experimental data. Two points require elaboration in this regard: first, the obvious discontinuity that exists at a velocity ratio of unity, and second, the necessity of expressing the velocity-ratio function as an absolute quantity to include the case of a faster moving inner stream.

The discontinuity at a velocity ratio of one is a direct consequence of the simplified mixing-length model used both in this report and quite generally in the literature. As a result, the model implies that a velocity ratio of one would result in no turbulence regardless of the initial Reynolds number of either stream. The model ascribes the presence of coaxial turbulence solely to the velocity difference between the two streams and does not allow for any turbulence initially present in either stream. Similarly, the model implies the existence of turbulence for velocity ratios greater than one for any Reynolds number. Although the initial flow might be sufficiently stable to damp out any turbulence initiated by the velocity difference at the stream interface, the model does not include such a possibility. The fact that the empirical correlation of the data required that the Reynolds number function take the form of $Re - 250$ probably reflects this deficiency in the model.

Since the flow model implies that coaxial turbulence is determined by the velocity ratio regardless of which stream velocity is larger, an absolute value of the outer- to inner-stream velocity-ratio function is necessary to avoid imaginary values of dimensionless eddy viscosity. The range of applicability of the correlation, however, must be identified in terms of the actual ratios of outer- to inner-stream velocities for which data were taken. The range of maximum to minimum velocity ratio was quite limited for the case of a faster moving inner stream. Finally, the applicability of the correlation is limited to initial bromine inner-stream Reynolds numbers greater than 255, the lowest experimental value.

The final correlation of the dimensionless eddy viscosity in terms of the initial bromine inner-stream Reynolds number and the initial outer- to inner-stream velocity ratio is, as given before,

$$\epsilon^+ = 0.0172\left|\bar{u}_2 - 1\right|^{1/2}(\mathrm{Re}_{1,0} - 250)$$

for $0.83 \leq \bar{u}_2 \leq 0.97$, $1.25 \leq \bar{u}_2 \leq 49$, and $255 \leq \mathrm{Re}_{1,0} \leq 3850$. These ranges, for the test-section dimensions used, imply an air (outer-stream) Reynolds number range of $1330 \leq \mathrm{Re}_2 \leq 49{,}300$.

SUMMARY OF RESULTS

The isothermal coaxial-flow system under investigation was formed by injecting a bromine stream into a surrounding air stream moving in the same direction. Optical measurements of the radial average bromine concentration were made at 1-inch intervals downstream from the point of injection. The data were compared with a laminar analysis that was modified to include turbulence effects by introducing a dimensionless eddy viscosity assumed to be radially and axially constant. Experimental data were obtained for air Reynolds numbers from 1330 to 49,300, bromine Reynolds numbers from 255 to 3850, and air-to-bromine initial-velocity ratios from 0.83 to 0.97 and 1.25 to 49. The results of this study are summarized as follows:

1. For the lowest attainable bromine Reynolds number (255), an air Reynolds number of 1730, and an initial-velocity ratio of 4.3, the measured axial variation of bromine concentration was in good agreement with the predicted laminar results.

2. For all other runs, the initial bromine Reynolds numbers were greater than 255, the air Reynolds numbers varied from 1330 to 49,300, and the data were not in agreement with laminar predictions.

3. Good agreement between analysis and experiment was obtained for all these runs by a trial and error selection of an eddy- to laminar-viscosity ratio ϵ^+ to modify the laminar results.

4. The dimensionless eddy viscosity ϵ^+ necessary to bring analysis and experiment into agreement was found to be represented by the following function of initial outer- to inner-stream velocity ratio $\bar{u}_2$ and initial bromine Reynolds number $\mathrm{Re}_{1,0}$:

$$\epsilon^+ = 0.0172\left|\bar{u}_2 - 1\right|^{1/2}(\mathrm{Re}_{1,0} - 250)$$

where $.83 \leq \bar{u}_2 \leq 0.97$, $1.25 \leq \bar{u}_2 \leq 49$, and $255 \leq \mathrm{Re}_{1,0} \leq 3850$.

Lewis Research Center
National Aeronautics and Space Administration
Cleveland, Ohio, October 17, 1963

REFERENCES

1. Jacobs, Paul F.: Turbulent Mixing in a Partially Ionized Gas. Rep. 625, Aero. Eng. Lab., Princeton Univ., Oct. 1962.

2. Weinstein, Herbert, and Ragsdale, Robert G.: A Coaxial Flow Reactor - A Gaseous Nuclear-Rocket Concept. Preprint 1518-60, Am. Rocket Soc., Inc., 1960.

3. Pai, Shih-I: Fluid Dynamics of Jets. Ch. IV, D. Van Nostrand Co., Inc., 1954.

4. Weinstein, Herbert, and Todd, Carroll, A.: A Numerical Solution of the Problem of Mixing of Laminar Coaxial Streams of Greatly Different Densities - Isothermal Case. NASA TN D-1534, 1963.

5. Burley, Richard R., and Bryant, Lively: Experimental Investigation of Coaxial Jet Mixing of Two Subsonic Streams at Various Temperature, Mach Number, and Diameter Ratios for Three Configurations. NASA MEMO 12-21-58E, 1959.

6. Landis, F., and Schapiro, A. H.: The Turbulent Mixing of Coaxial Gas Jets. Heat Transfer and Fluid Mech. Inst., Stanford Univ. Press, 1951, pp. 133-146.

7. Squire, H. B., and Trouncer, J.: Round Jets in a General Stream. R & M 1974, British ARC, 1944.

8. Schlinger, W. G., and Sage, B. H.: Material Transfer in a Turbulent Air Stream. Prog. Rep. 4-108, Jet Prop. Lab., C.I.T., Oct. 1949.

9. Shapiro, Archer H.: Turbulent Transfer Processes in Parallel Jets. Hydrodynamics in Modern Tech., Hydrodynamics Lab., M.I.T., 1951, pp. 141-146.

10. Ragsdale, Robert G., and Weinstein, Herbert: On the Hydrodynamics of a Coaxial Flow Gaseous Reactor. Proc. ARS/ANS/IAS Nuclear Prop. Conf., Aug. 1962, TID 7653, pt. 1, pp. 82-88.

11. Hirschfelder, Joseph O., Curtiss, Charles F., and Bird, R. Byron: Molecular Theory of Gases and Liquids. John Wiley & Sons, Inc., 1954.

12. Sherwood, T. K.: Absorption and Extraction. McGraw-Hill Book Co., Inc., 1937, p. 18.

13. Perry, J. H., ed.: Chemical Engineers' Handbook. Third ed., McGraw-Hill Book Co., Inc., 1950, p. 371.

14. Schlichting, Hermann: Boundary Layer Theory. Fourth ed., McGraw-Hill Book Co., Inc., 1960.

TABLE I. - AIR-BROMINE COAXIAL-FLOW DATA

Run	Flow rate, lb/sec		Velocity, ft/sec		Pressure, lb/sq in. abs	Turbulence factor, ϵ^+	Reynolds number	
	Air	Bromine	Air	Bromine			Air	Bromine
1	0.0074	0.000288	1.81	2.18	4.86	6	1,350	1030
2	.0073	.000250	1.79	1.85	4.86	6	1,330	870
3	.00945	.000244	2.8	2.24	4.03	6	1,720	870
4	.0095	.000187	2.81	1.71	4.03	5	1,730	670
5	.0095	.0000716	2.54	.59	4.43	0	1,730	255
6	.0313	.000336	7.97	2.83	4.62	35	5,680	1200
7	.0475	.00108	13.1	9.25	4.26	35	8,680	3850
8	.0475	.000892	13.1	7.62	4.26	43	8,680	3190
9	.0475	.000731	13.1	6.24	4.26	35	8,680	2610
10	.0475	.000529	13.1	4.52	4.26	30	8,680	1920
11	.091	.000852	24.7	7.16	4.42	80	16,600	3060
12	.091	.000666	24.7	5.6	4.42	65	16,600	2370
13	.091	.000370	24.7	3.11	4.42	40	16,600	1310
14	.091	.000245	24.7	2.06	4.42	35	16,600	870
15	.15	.000824	40.8	6.94	4.42	120	27,400	2930
16	.152	.000532	41.3	4.48	4.42	80	27,700	1900
17	.147	.000245	40.0	2.06	4.42	55	27,000	875
18	.247	.000882	72.7	8.04	4.08	140	45,100	3150
19	.267	.000726	75.6	6.36	4.26	125	48,400	2590
20	.267	.000487	75.6	4.27	4.26	100	48,400	1730
21	.272	.000179	77.1	1.57	4.26	60	49,300	640

TABLE II. - NORMALIZED BROMINE CONCENTRATION

Run	Axial distance, $\bar{z}$							
	0.29	4.65	9.3	13.95	18.6	23.3	27.9	32.6
1	1.0	0.69	0.62	0.51	0.51	0.40	0.42	0.33
2	1.0	.58	.56	.43	.36	.33	.32	.28
3	1.0	.62	.57	.45	.41	.35	.29	.29
4	1.0	.52	.47	.36	.33	.27	.26	.24
5	1.0	.37	.44	---	.35	.24	.21	.15
6	1.0	.33	.28	.14	.12	.10	.075	.047
7	1.0	.65	.72	---	.51	.42	.34	.31
8	1.0	.58	.62	---	.36	.28	.25	.22
9	1.0	.57	.60	---	.33	.26	.22	.20
10	1.0	.50	.44	---	.22	.18	.16	.14
11	1.0	.47	.27	.17	.12	.10	.091	.086
12	1.0	.40	.22	.13	.11	.094	.075	.074
13	1.0	.31	.16	.088	.074	.061	.055	.053
14	1.0	.21	.12	.081	.056	.049	.038	.031
15	1.0	.28	.15	.11	.084	.076	.071	.064
16	1.0	.19	.11	.079	.055	.053	.050	.046
17	1.0	.11	.065	.047	.040	.033	.029	.026
18	1.0	.18	.11	.074	.064	.055	.048	.048
19	1.0	.15	.10	.066	.094	.050	.060	.056
20	1.0	.090	.061	.044	.035	.030	.030	.029
21	1.0	.035	.024	.020	.014	.014	.014	.012

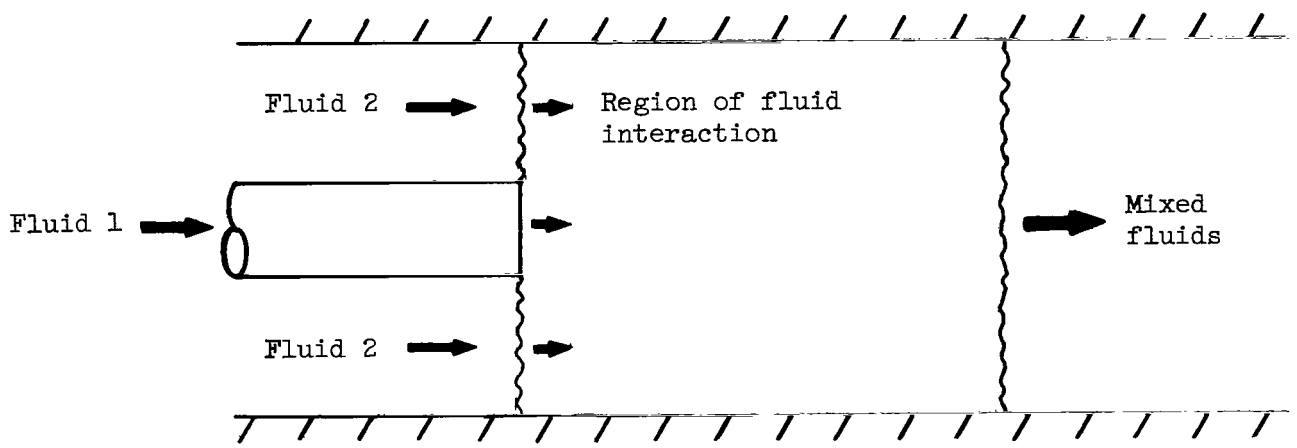

Figure 1. - General flow system under investigation.

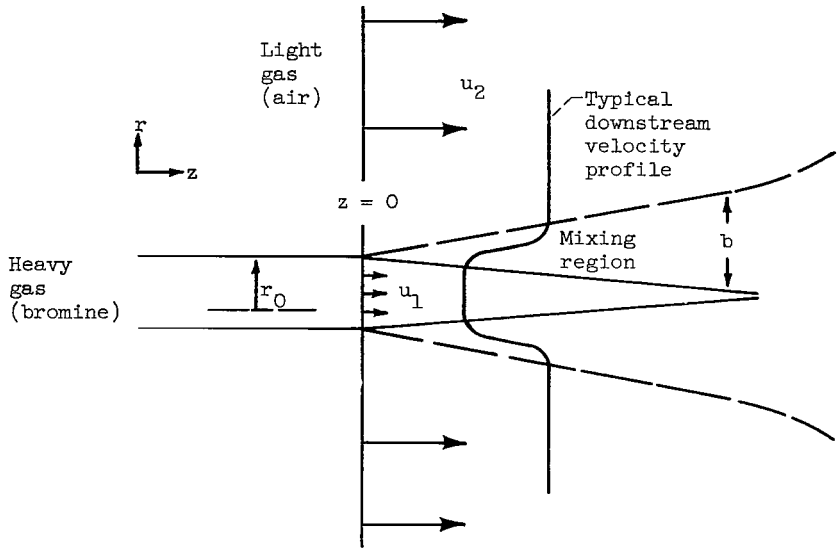

Figure 2. - Coaxial-flow model for analysis.

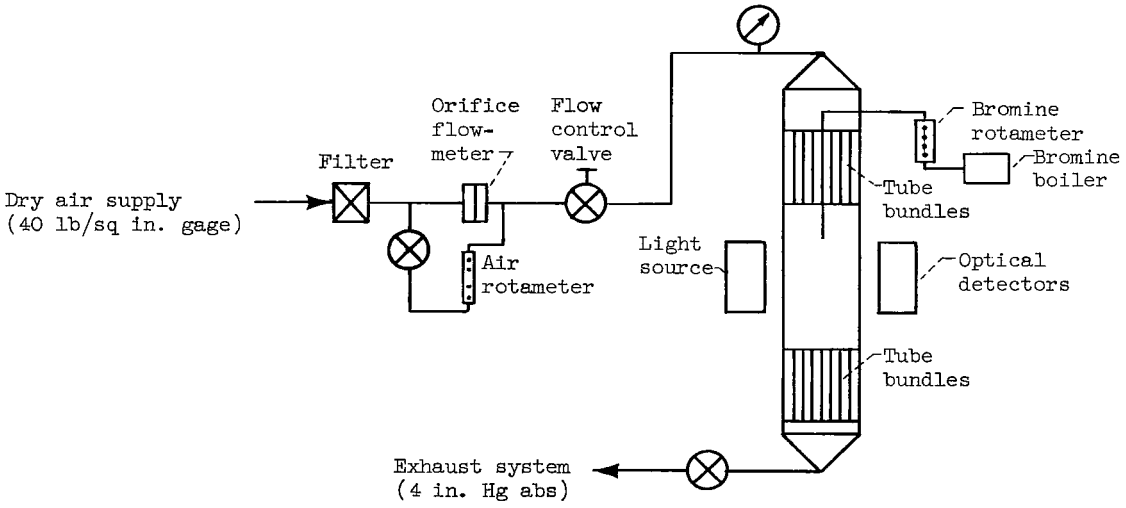

Figure 3. - Schematic drawing of air-bromine system.

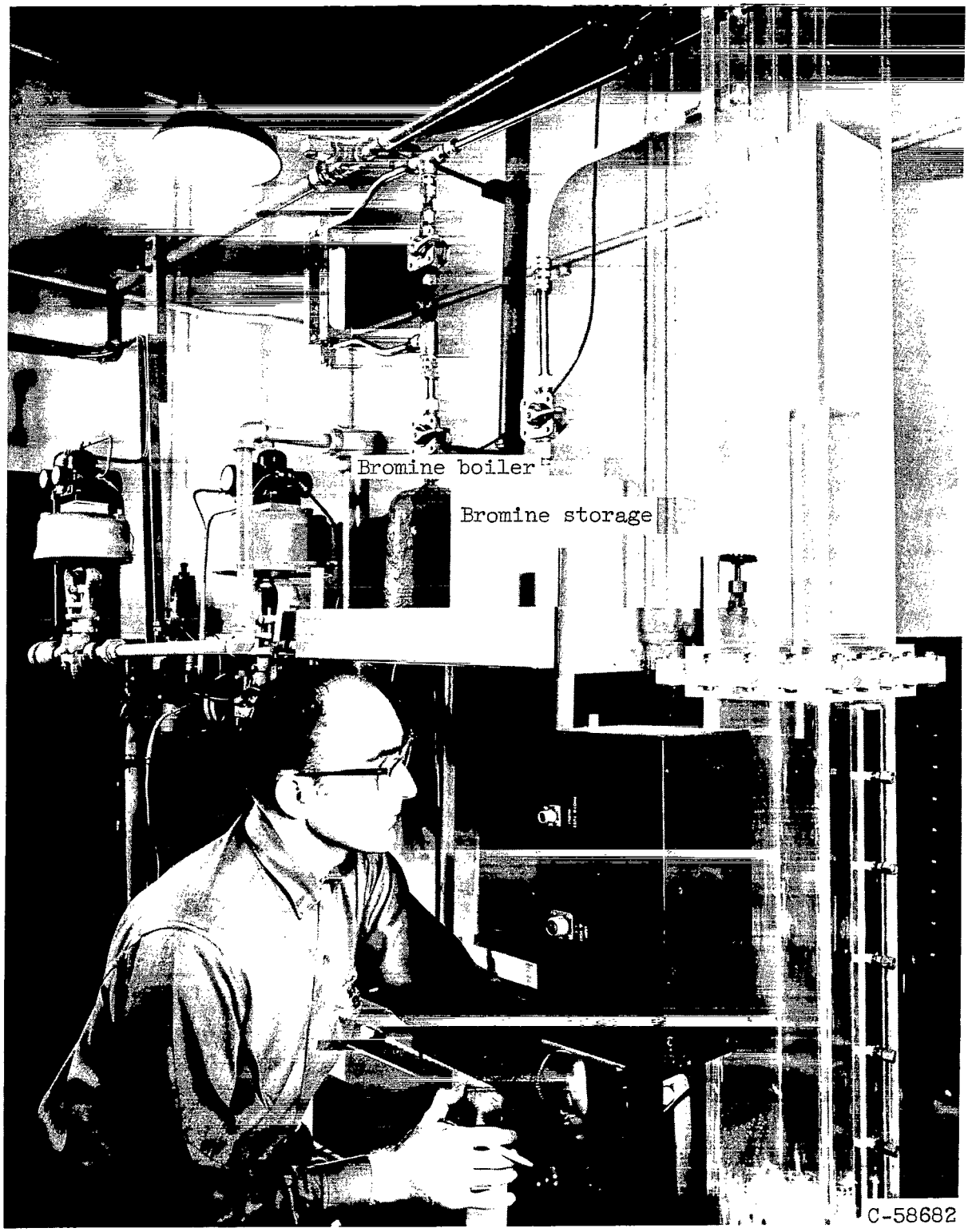

Figure 4. - Air-bromine experimental apparatus.

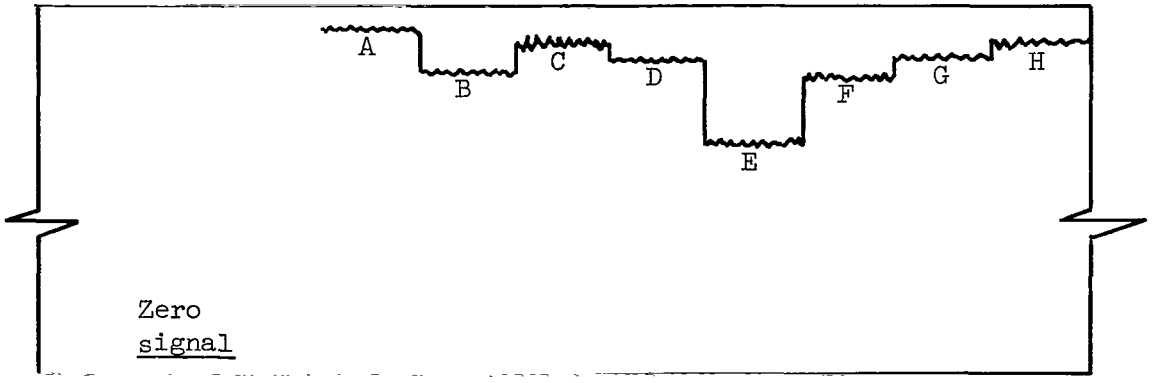

(a) Full-scale deflection (no bromine flow).

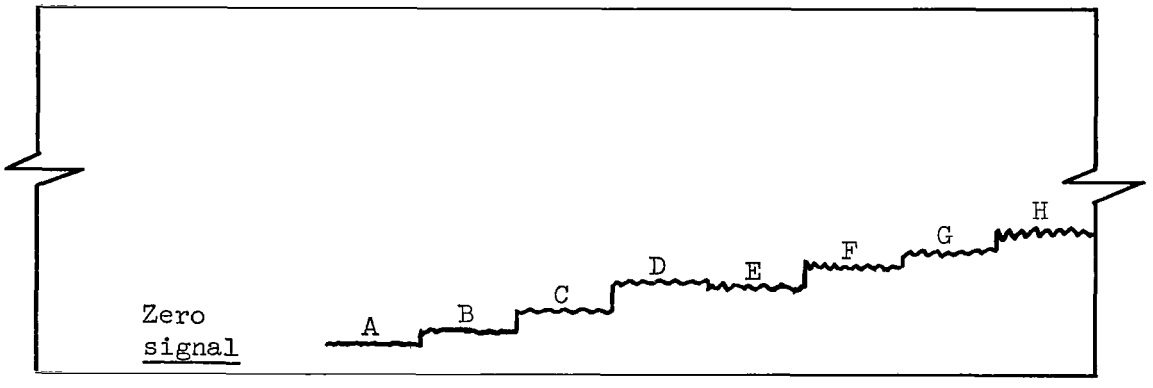

(b) Attenuated deflection (bromine flow).

Figure 5. - Oscillograph traces for photomultiplier stations A to H.

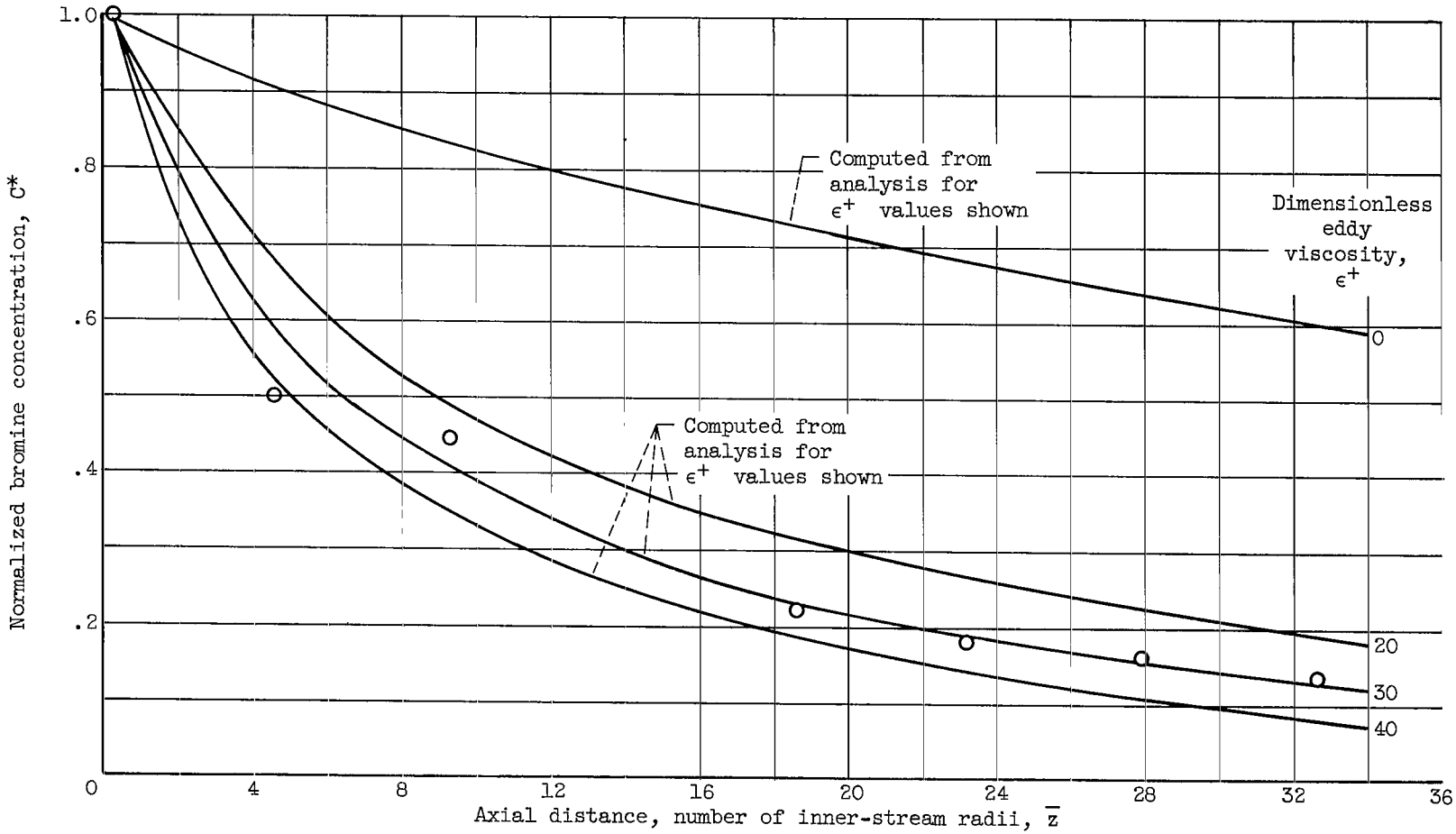

Figure 6. - Sensitivity of analysis to dimensionless eddy viscosity ϵ^+ for initial bromine Reynolds number of 1920, air Reynolds number of 8680, and air-to-bromine initial-velocity ratio of 2.9 (run 10).

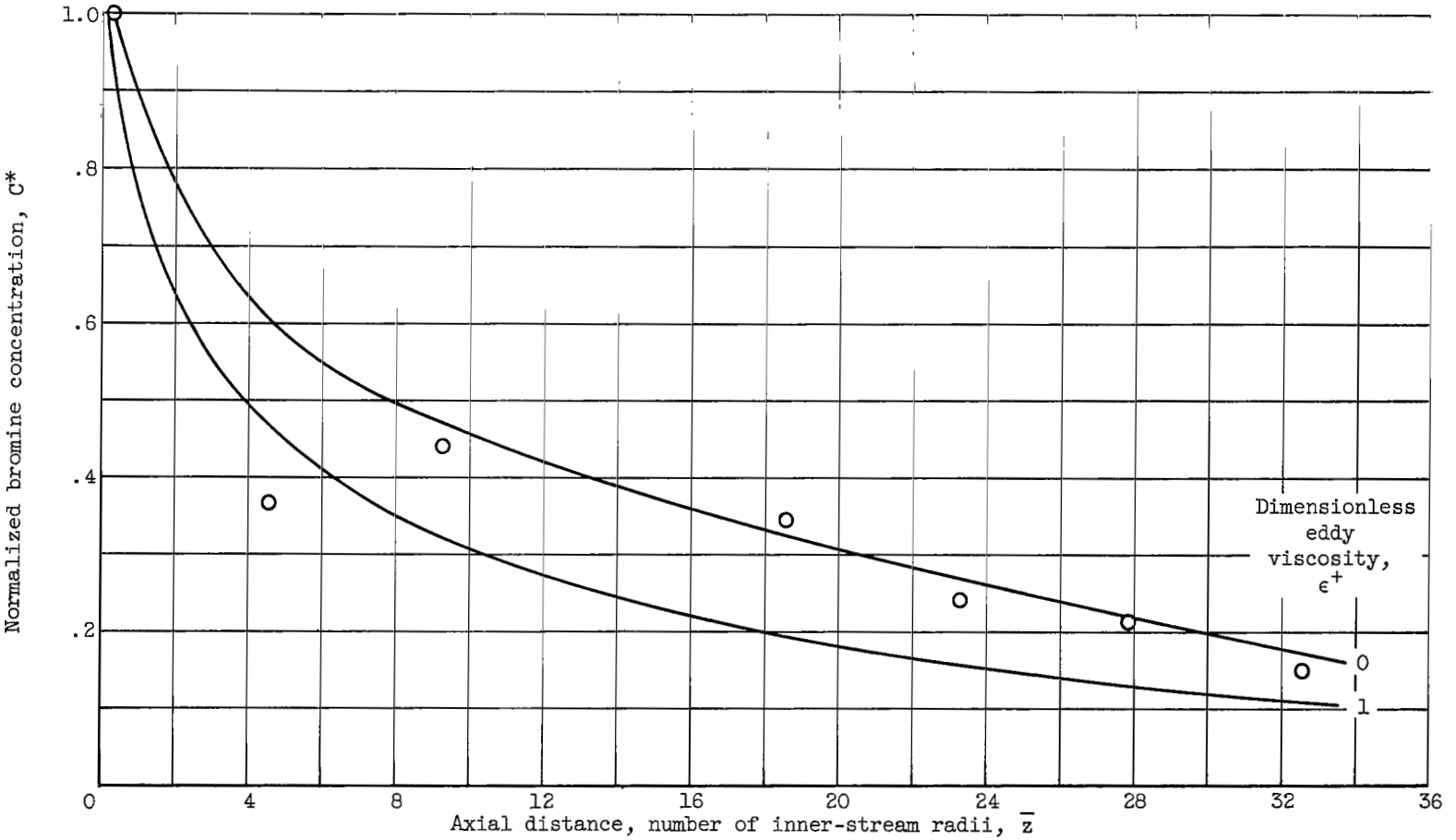

Figure 7. - Laminar flow data for air Reynolds number of 1730, bromine Reynolds number of 255, and initial-velocity ratio of 4.3 (run 5).

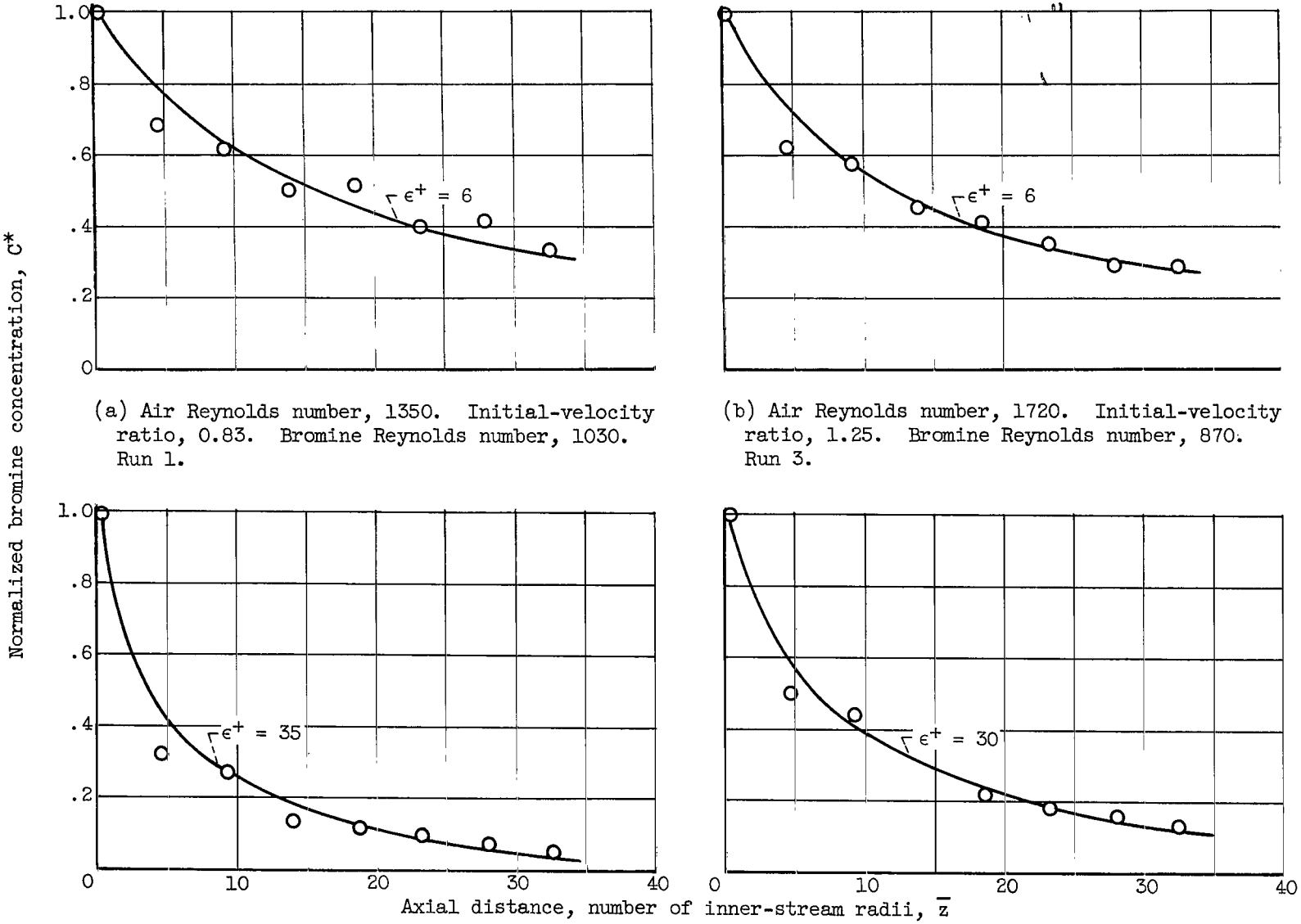

(a) Air Reynolds number, 1350. Initial-velocity ratio, 0.83. Bromine Reynolds number, 1030. Run 1.

(b) Air Reynolds number, 1720. Initial-velocity ratio, 1.25. Bromine Reynolds number, 870. Run 3.

(c) Air Reynolds number, 5680. Initial-velocity ratio, 2.8. Bromine Reynolds number, 1200. Run 6.

(d) Air Reynolds number, 8680. Initial-velocity ratio, 2.9. Bromine Reynolds number, 1920. Run 10.

Figure 8. - Turbulent flow data.

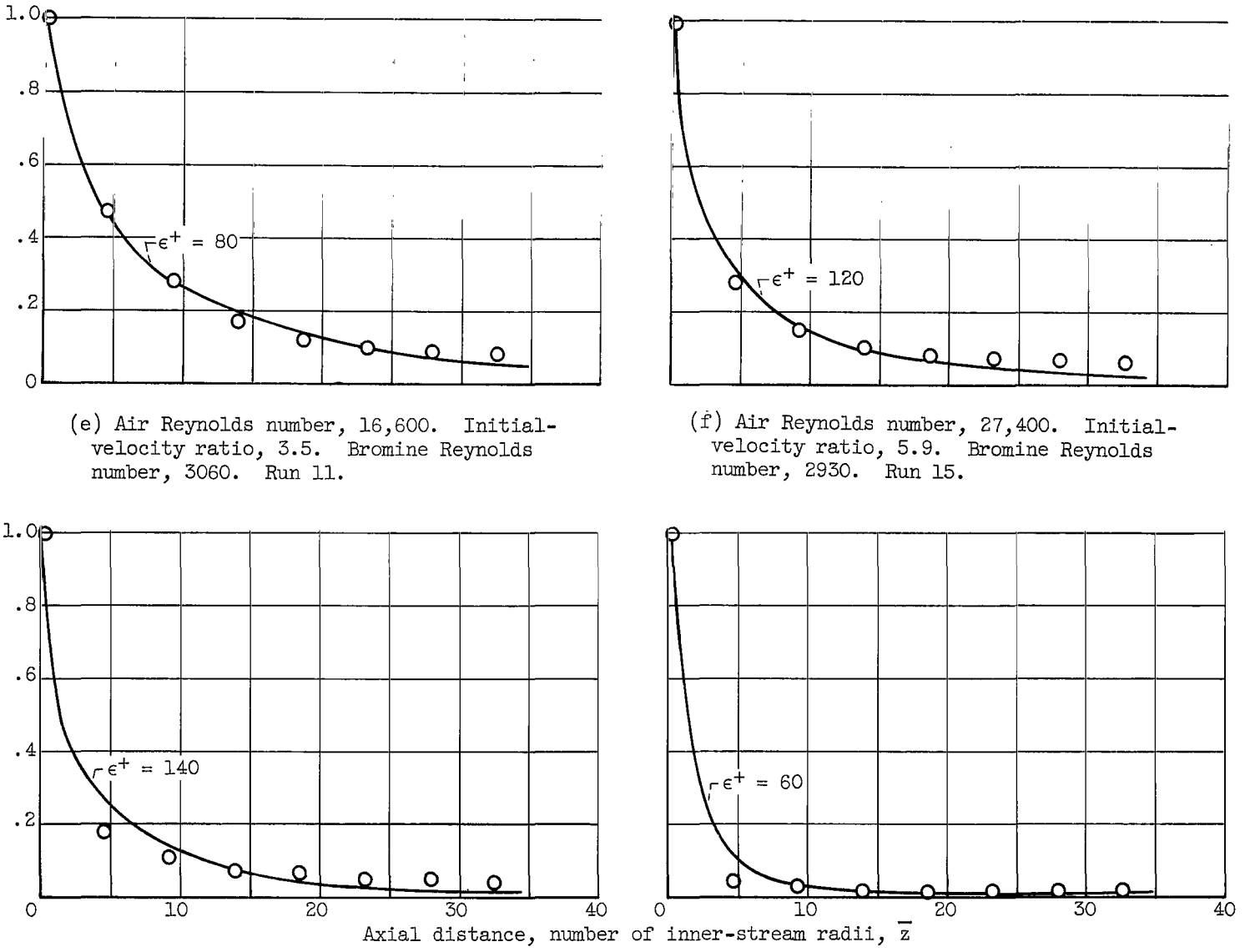

(e) Air Reynolds number, 16,600. Initial-velocity ratio, 3.5. Bromine Reynolds number, 3060. Run 11.

(f) Air Reynolds number, 27,400. Initial-velocity ratio, 5.9. Bromine Reynolds number, 2930. Run 15.

(g) Air Reynolds number, 45,100. Initial-velocity ratio, 9. Bromine Reynolds number, 3150. Run 18.

(h) Air Reynolds number, 49,300. Initial-velocity ratio, 49. Bromine Reynolds number, 640. Run 21.

Figure 8. - Concluded. Turbulent flow data.

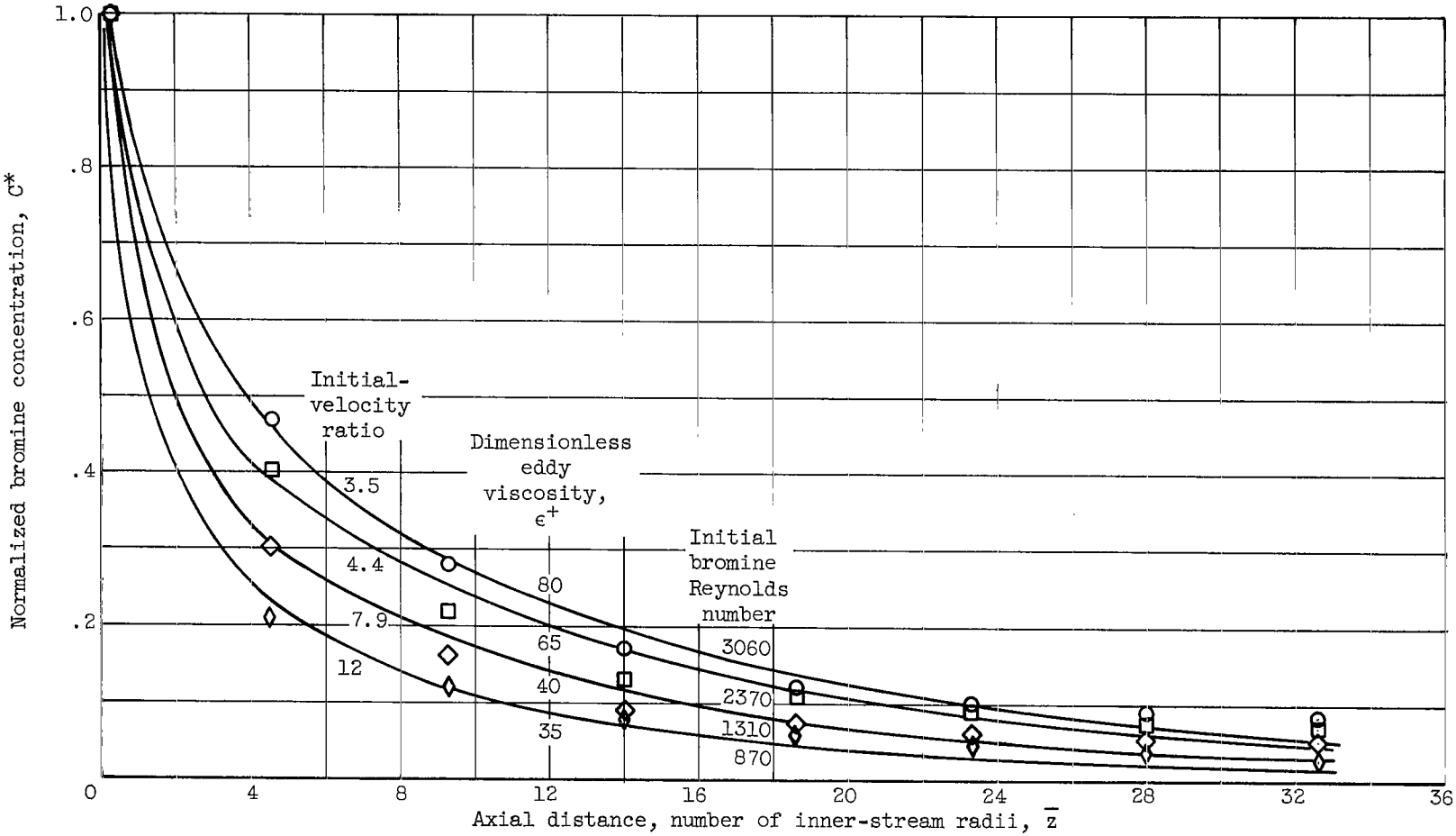

(a) Constant air Reynolds number, 16,600.

Figure 9. - Effect of initial-velocity ratio.

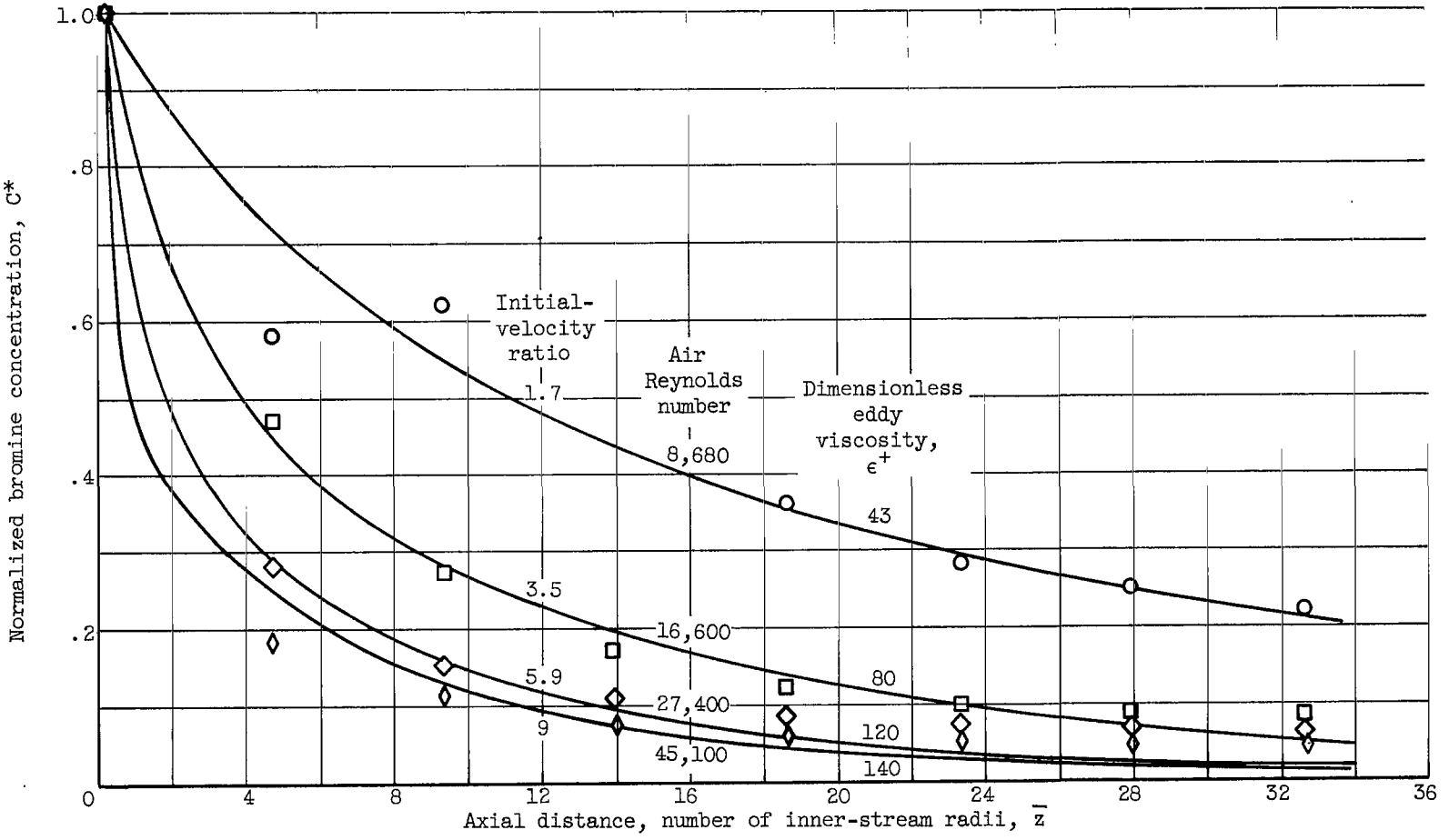

(b) Approximately constant initial bromine Reynolds number, 2930-3190.

Figure 9. - Concluded. Effect of initial velocity ratio.

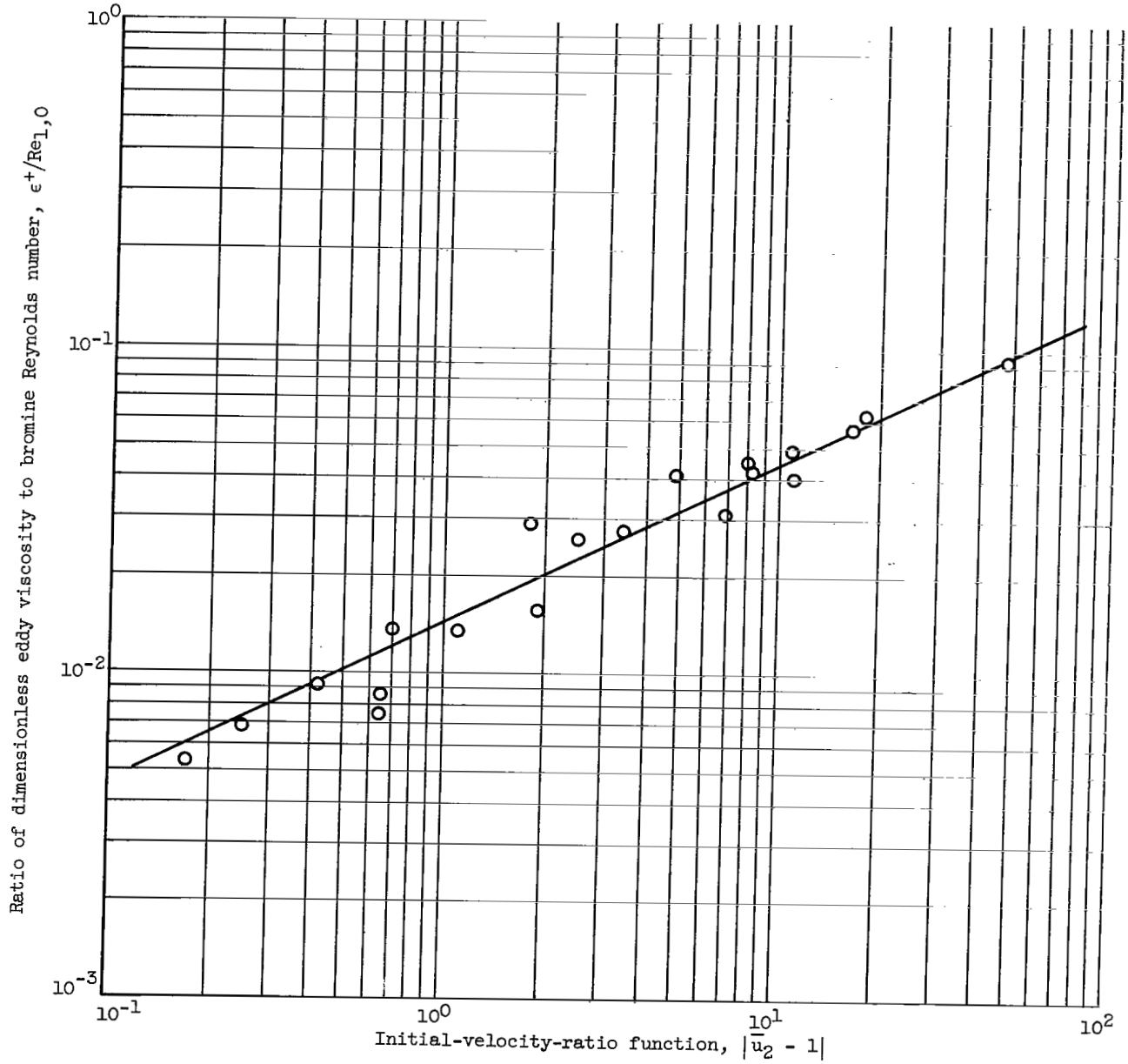

Figure 10. - Variation of initial-velocity ratio with $(\epsilon^+/Re_{1.0})$.

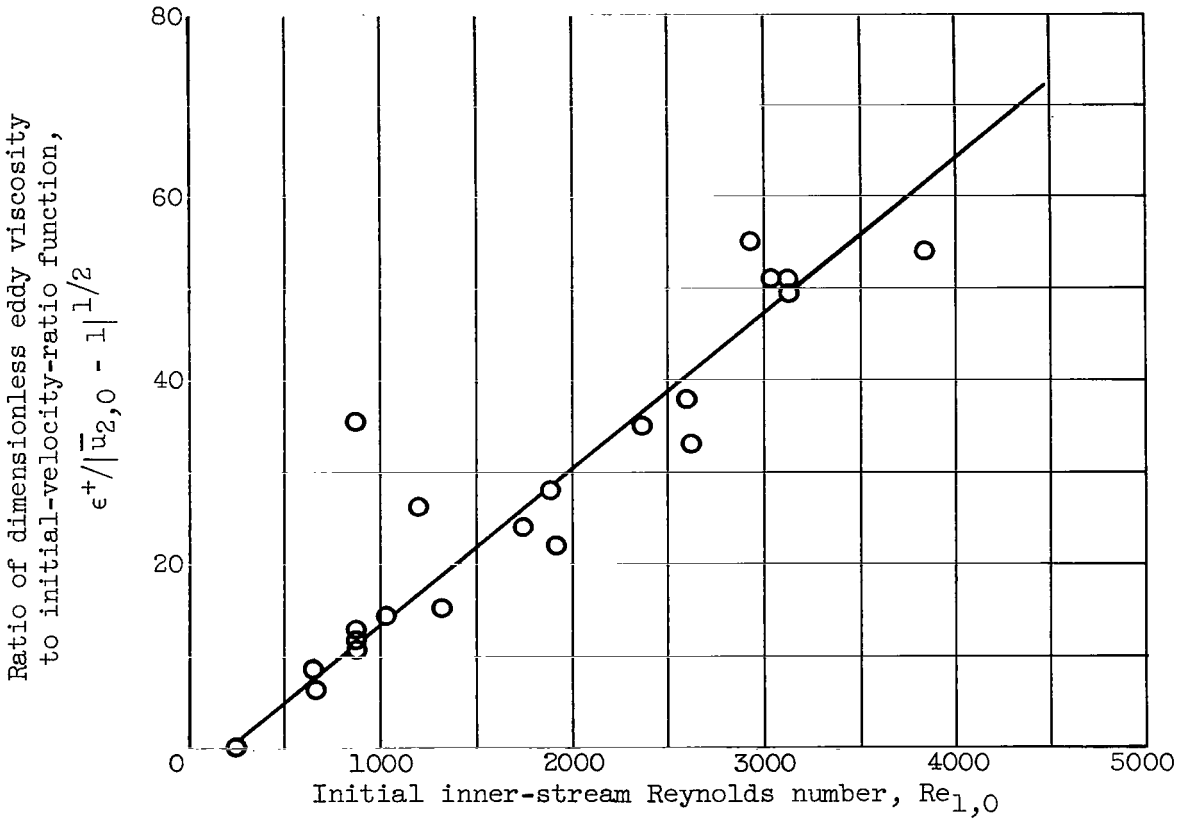

Figure 11. - Effect of initial inner-stream Reynolds number.

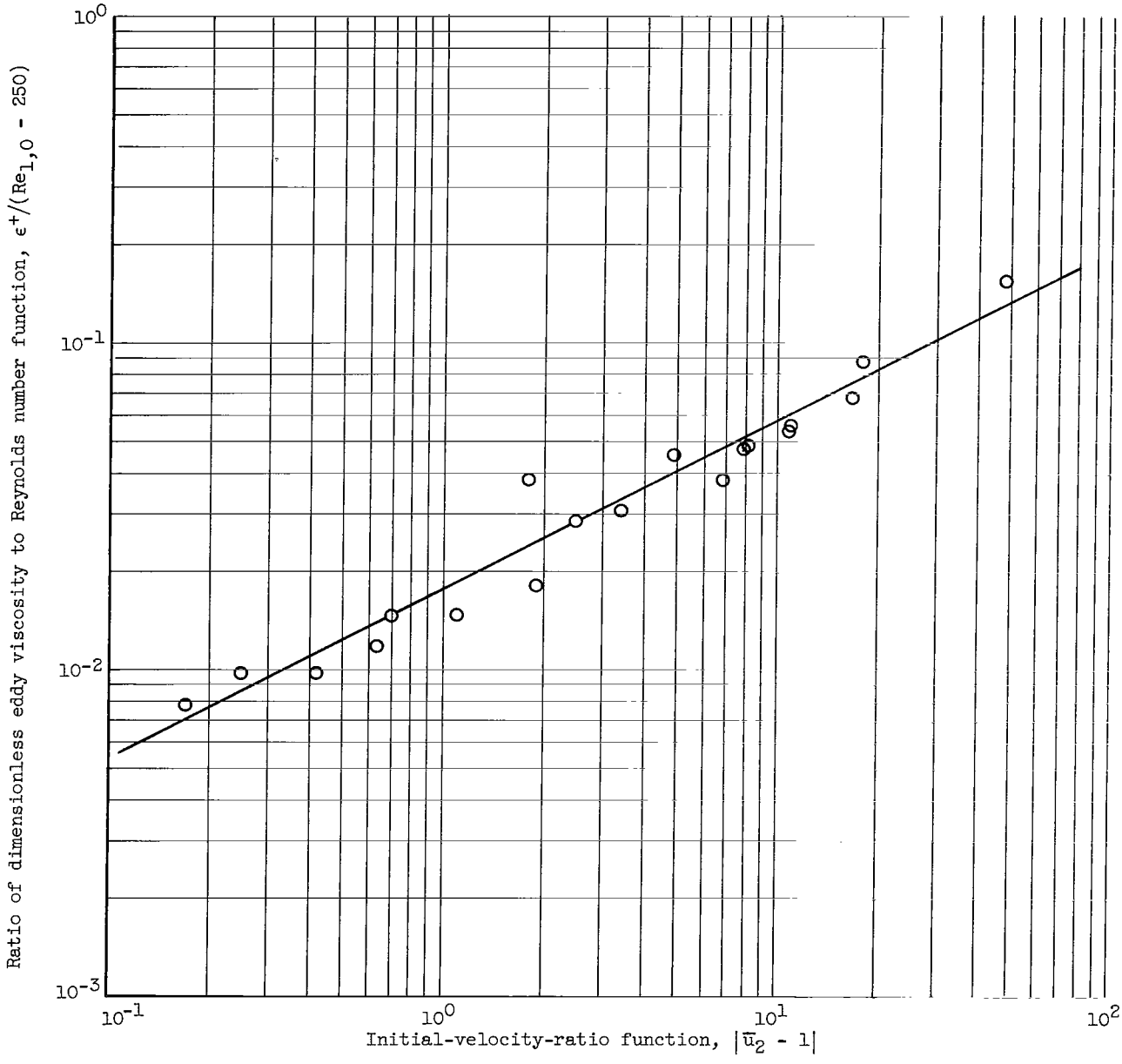

Figure 12. - Variation of initial-velocity-ratio function with $\epsilon^+/(Re_{1,0} - 250)$.

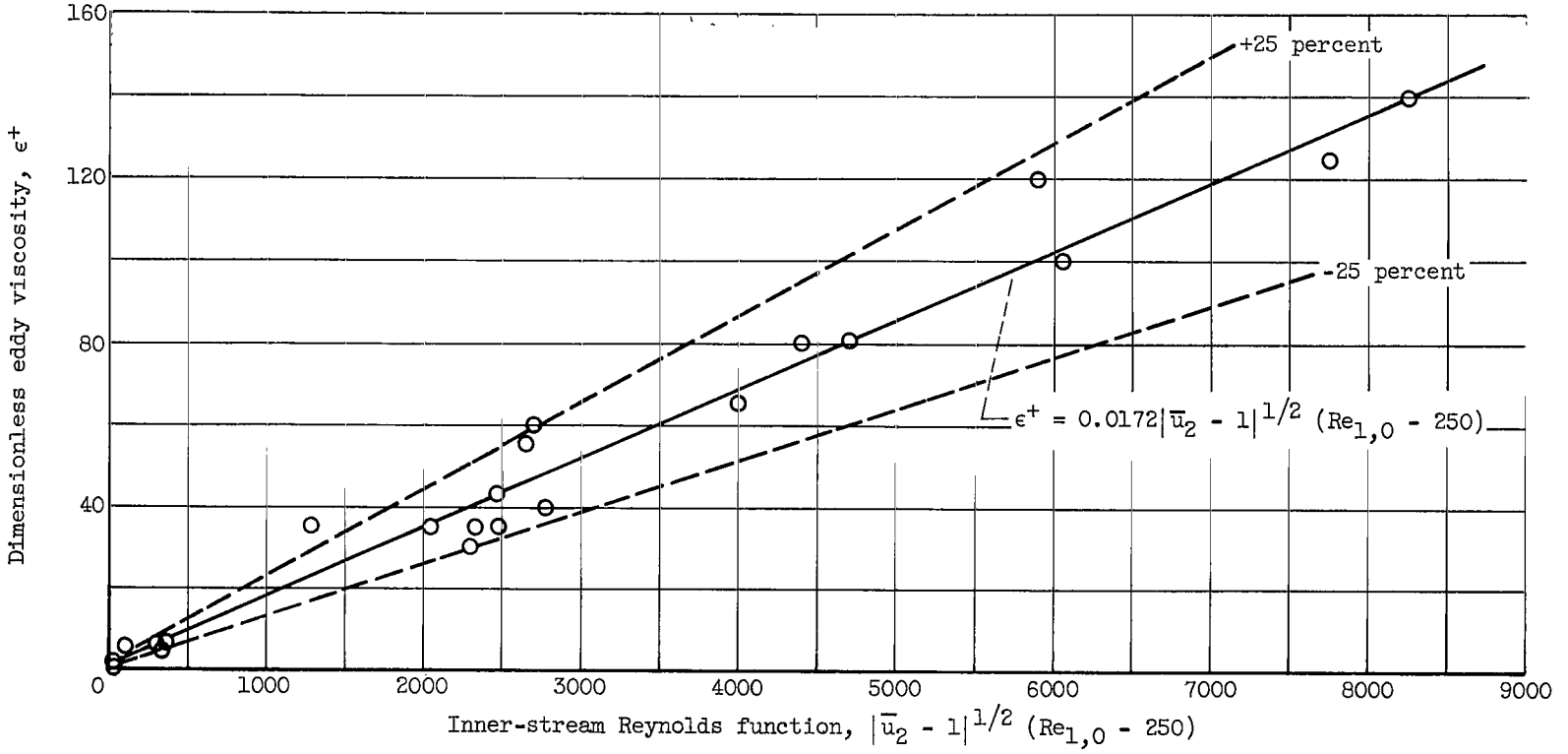

Figure 13. - Final correlation of data.